Acta Crystallographica Section D
Biological Crystallography
ISSN 0907-4449

Three-dimensional structures of L-asparaginase from *Erwinia carotovora* complexed with aspartate and glutamate

O. V. Kravchenko,[a] Yu. A. Kislitsin,[b] A. N. Popov,[b,c] S. V. Nikonov[a] and I. P. Kuranova[b]*

[a]Institute of Protein Research, Russian Academy of Sciences, 142290 Pushchino, Moscow Region, Russia, [b]Institute of Crystallography, Russian Academy of Sciences, Leninski Prospect 59, 119333 Moscow, Russia, and [c]European Synchrotron Radiation Facility, BP-220, F-38043 Grenoble CEDEX 09, France

Correspondence e-mail: inna@ns.crys.ras.ru

Received 2 October 2007
Accepted 5 December 2007

PDB References: L-asparaginase, L-aspartate complex, 2gvn, r2gvnsf; L-glutamate complex, 2hln, r2hlnsf.

The crystal structures of *Erwinia carotovora* L-asparaginase complexed with L-aspartate and L-glutamate were determined at 1.9 and 2.2 Å, respectively, using the molecular-replacement method and were refined to *R* factors of about 21% in both cases. The positions of the ligands in the active site were located. A comparison of the new structures with the known structures of *Escherichia coli* L-asparaginase and *Er. chrysanthemi* L-asparaginase was performed. It was found that the arrangement of the ligands practically coincides in all three enzymes. The peculiarities of the quaternary structure of the enzyme, the possible role of water molecules in the enzyme action and the conformational changes during the catalyzed reaction are discussed.

1. Introduction

L-Asparaginase from *Erwinia carotovora* (ErcA; L-asparagine amidohydrolase; EC 3.5.1.1) belongs to the family of highly homologous bacterial threonine amidohydrolases and predominantly utilizes L-asparagine as a substrate (Howard & Carpenter, 1972). A remarkable feature of bacterial L-asparaginases is their pronounced antitumour activity. Some of these enzymes have found wide application in medicine as effective antitumour agents for the treatment of acute lymphoblastic leukaemia, lymphosarcomas and reticulum cell sarcomas (Hortobagyi *et al.*, 1980; Roberts *et al.*, 1979; Carlsson *et al.*, 1995). The antitumour effect of L-asparaginases is attributed to their ability to suppress asparagine metabolism, which is necessary for tumour-cell growth (Rohm & Van Etten, 1986).

The antitumour activity of L-asparaginases is accompanied by a variety of side effects because of their intrinsic toxicity, which is particularly associated with the presence of glutaminase activity (Wo *et al.*, 1978). L-Glutamine is important in nitrogen transportation in the blood and prolonged depletion of this amino acid during asparaginase therapy causes serious biochemical disorders in the body. As a consequence, only two L-asparaginases, those from *Er. chrysanthemi* (ErchA) and *Escherichia coli* (EcA), which have the lowest glutaminase activity, have been used successfully as drugs (Derst *et al.*, 2000). In this regard, the search for and engineering of new enzymes that are effective as therapeutic agents is of special interest.

The biochemical properties and three-dimensional structures of several bacterial L-asparaginases and their complexes with substrates and inhibitors have been determined (Miller *et al.*, 1993; Lubkowski *et al.*, 1994, 1996; Swain *et al.*, 1993;

Polikarpov *et al.*, 1999). The results of kinetic measurements indicate that the enzymatic reaction catalysed by L-asparaginases proceeds *via* a covalent intermediate, probably a β-aspartyl enzyme. One of the threonine residues in the active site serves as a primary nucleophile. The suggested mechanism was confirmed by NMR studies of the oxygen-exchange reaction between bulk solvent and the side-chain carboxylate of aspartate as well as by results of the X-ray studies (Rohm & Van Etten, 1986; Palm *et al.*, 1996).

The recombinant enzyme from ErcA has 75 and 45% sequence identity to ErchA and EcA, respectively (Wikman *et al.*, 2005). Despite the high degree of homology between the L-asparaginases from the *Erwinia* strains and from *E. coli*, they differ remarkably in the relative magnitudes of their glutaminase and asparaginase activities. In comparison with the enzymes from *E. coli* and *Er. chrysanthemi*, recombinant *Er. carotovora* L-asparaginase possesses a relatively low glutaminase activity and shows a different antigenic specificity (Howard & Carpenter, 1972; Krasotkina *et al.*, 2004). As a result, ErcA could provide a therapy for patients with hypersensitivity to other asparaginases (Krasotkina *et al.*, 2004). These properties of recombinant L-asparaginase from *Er. carotovora* make this enzyme a good candidate for therapeutic and protein-engineering use.

Table 1
Data-collection and refinement statistics.

Values in parentheses are for the highest resolution shell.

Structure	ErcAA, 1.9 Å	ErcAA, 2.1 Å	ErcAG
Data-collection statistics			
Space group	$P2_12_12_1$	$P2_1$	$P2_1$
Unit-cell parameters			
a (Å)	73.06	123.04	81.11
b (Å)	135.88	73.03	123.68
c (Å)	251.53	140.35	197.45
α (°)	90.00	90.00	90.00
β (°)	90.00	105.17	90.92
γ (°)	90.00	90.00	90.00
Wavelength (Å)	0.98	0.98	0.99
Resolution (Å)	20.00–1.90 (1.92–1.90)	20.00–2.10 (2.12–2.10)	20.00–2.20 (2.22–2.20)
No. of reflections	707307	306886	593680
No. of unique reflections	191790 (5744)	121753 (2884)	180862 (5910)
Completeness (%)	97.2 (88.1)	86.7 (62.3)	91.8 (91.0)
Average redundancy	3.3 (3.2)	2.5 (2.0)	3.3 (3.3)
$I/\sigma(I)$	31.3 (5.5)	26.8 (2.9)	17.2 (2.6)
Refinement statistics			
Resolution range (Å)	14.99–1.90	15.36–2.10	19.98–2.20
No. of reflections	181808	115200	170479
R factor (%)	20.4	18.7	22.0
Free R factor (%)	22.9	25.00	26.7
R.m.s. deviation from ideal			
Bond lengths (Å)	0.007	0.008	0.005
Bond angles (°)	0.941	0.921	0.919
Mean B value overall (Å^2)	27.1	40.7	43.1
Content of the asymmetric unit			
Amino-acid residues	2600	2600	2600
Ligand molecules	8	8	12
Water O atoms	2301	1303	1873
PDB code	2gvn	—	2hln

L-Asparaginases function as a homotetramer (Lubkowski *et al.*, 1994). The tetrameric molecule of the enzyme, which has approximate 222 symmetry, contains four active sites, each of which contains amino-acid residues from two neighbouring subunits. The latter form a so-called intimate dimer and the whole molecule can be considered as a dimer of dimers (Swain *et al.*, 1993; Lubkowski *et al.*, 1994).

The determination of the three-dimensional structure of L-asparaginase from *E. coli* with bound aspartic acid allowed location of the active-site cavity and identification of the amino-acid residues situated in the vicinity of the ligand and shed light on the structural basis of the specificity of these enzymes (Swain *et al.*, 1993; Aghaiypour *et al.*, 2001*a*).

Here, we present the three-dimensional structures of *Er. carotovora* L-asparaginase in complexes with L-aspartate at 1.9 Å and with L-glutamate at 2.2 Å resolution. Bound ligands were located in all four active sites of the enzyme molecule. The positions of the ligands were found to be very similar in the highly homologous asparaginases from *E. coli*, *Er. chrysanthemi* and *Er. carotovora*. We considered the peculiarities of the quaternary structure of the enzyme, which are significant for the activity of the enzyme, the possible role of the water molecules nearest to the bound ligand in the action of the enzyme and the conformational changes that accompany the catalyzed reaction.

2. Materials and methods

2.1. Crystallization

A sample of recombinant L-asparaginase purified according to the method of Krasotkina *et al.* (2004) was kindly supplied by Professor N. N. Sokolov (Institute of Biomedical Chemistry, Russian Academy of Medical Sciences).

Crystals of complexes of ErcA with L-aspartic acid (ErcAA) and L-glutamic acid (ErcAG) were grown by the hanging-drop vapour-diffusion technique at 295 K from 20 mg ml^{-1} enzyme solution in 0.1 *M* sodium cacodylate buffer pH 5.0 containing 20 m*M* aspartate (or glutamate) and 0.03% β-octylglucoside. 12% PEG MME 5000 in 0.1 *M* sodium cacodylate buffer pH 5.0 was used as a precipitant. Crystals appeared after 5–6 d and reached dimensions of 0.1 × 0.2 × 0.3 mm after two weeks. Larger isometric crystals were grown using microseeding (Stura & Wilson, 1991). A cat's whisker was placed into a protein-solution drop to touch the crystal. The adsorbed microseeds were transferred into a protein/precipitant drop previously equilibrated with reservoir solution with a reduced precipitant concentration. Crystals appeared overnight and reached dimensions of 0.4 × 0.4 × 0.7 mm after 2–3 d. The

crystals of ErcA complexed with aspartate belonged to space groups $P2_12_12_1$ and $P2_1$ and diffracted to 1.9 and 2.1 Å, respectively. Crystals of ErcA complexed with L-glutamate belonged to space group $P2_1$ and diffracted to 2.2 Å.

2.2. Data collection and processing

All X-ray data were collected on beamline BW7A at EMBL Hamburg, c/o DESY, Germany using a MAR Research CCD detector. The crystals were flash-cooled to 100 K in a nitrogen-gas stream. Prior to flash-freezing, the crystals were soaked for a short time in reservoir solution supplemented with 15% glycerol as a cryoprotectant. The data were processed and merged with *DENZO* and *SCALEPACK* (Otwinoski & Minor, 1997). Data-collection statistics are presented in Table 1.

2.3. Structure solution and refinement

The ErcAA and ErcAG structures were solved by the molecular-replacement method using the *CCP*4 (Collaborative Computational Project, Number 4, 1994) version of *AMoRe* (Navaza, 1994) and *Phaser* (Storoni *et al.*, 2004) with the structure of free L-asparaginase from *Er. carotovora* (PDB code 1zcf) as a search model.

Eight copies of the ErcA subunit were placed into the asymmetric part of the unit cell of the ErcAA crystal. They form two homotetrameric molecules: the *ABEF* and *CDGH* tetramers. The Matthews coefficient (V_M) was 2.26 Å^3 Da^{-1}, corresponding to a solvent content of 45.5%. The crystallographic asymmetric unit of ErcAG contains 12 subunits, with a V_M of 2.39 Å^3 Da^{-1} and a solvent content of 48.5%.

Molecular replacement yielded an unambiguous solution with a correlation coefficient of 71.1% and an R factor of 41.7% for the rhombohedral ErcAA crystals and with a correlation coefficient of 71.5% and an R factor of 32.9% for the monoclinic crystals. The structure of ErcAG was solved using the *Phaser* program. The LLG value was 37 372.

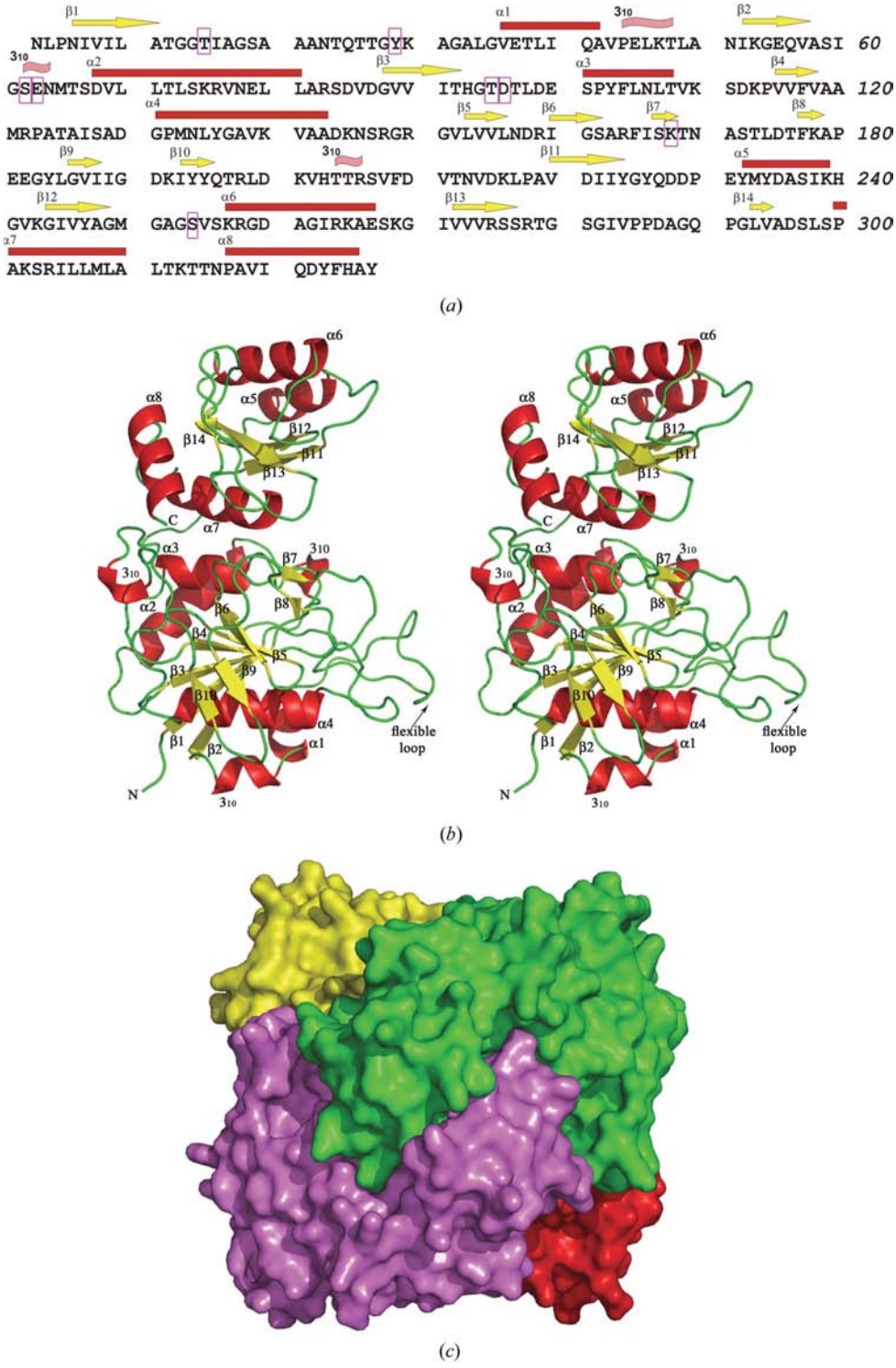

Figure 1
(*a*) Amino-acid sequence of ErcA. Secondary-structure elements are represented graphically above the alignment. α-Helices are shown as red rectangles and β-strands as yellow arrows. The amino-acid residues of the active site are shown in frames. (*b*) Stereoview of a ribbon diagram of the ErcA subunit; α-helices (red) and β-strands (yellow) are numbered. (*c*) Tetrameric molecule of ErcA. Subunits *A*, *B*, *E* and *F* are shown in yellow, green, red and violet.

The programs *CNS* (Brünger *et al.*, 1998) and *REFMAC* (Murshudov *et al.*, 1999) were used for structure refinement. Each subunit in the asymmetric unit was refined separately. The progress of the refinement was monitored by using 5% of the reflections to calculate an $R_{\rm free}$ factor. The electron-density map calculations were performed with *CNS* and *CCP*4. For map interpretation and model building, the programs *O* (Jones *et al.*, 1991) and *Coot* (Emsley & Cowtan, 2004) were used.

Despite the high quality of the electron-density maps, it was impossible to distinguish the positions of the first two N-terminal residues in all three structures and of amino-acid residues 18–34 in the electron-density map of ErcAG. The substrate-binding sites were easily found by manual inspection of the electron-density maps. Substrate and water molecules were added to the models and this was followed by several cycles of refinement.

The stereochemical parameters of the models were tested using *PROCHECK* (Laskowski *et al.*, 1993) and *WHAT-CHECK* (Hooft *et al.*, 1996). All three models were of good quality; nevertheless, two residues (Asp296 and Thr204) of each monomer were located in disallowed regions of the Ramachandran plot. A similar arrangement of these residues is characteristic of homologous asparaginases of known structure (Swain *et al.*, 1993; Lubkowski, Wlodawer, Ammon *et al.*, 1994; Lubkowski, Wlodawer, Housset *et al.*, 1994; Lubkowski *et al.*, 1996, 2003).

Data-collection and refinement statistics are summarized in Table 1. Several peaks in the electron-density map of ErcAG were interpreted as short PEG molecules. The final model of *Er. carotovora* L-asparaginase in complex with glutamic acid contains eight PEG molecules. The O atoms of the PEG molecules form hydrogen bonds to ErcAG. The PEG molecules are found on the enzyme surface or in the cavities between the enzyme subunits. In some cases L-asparaginase subunits make contacts with each other *via* PEG molecules.

Intermolecular and intersubunit contacts were calculated for both crystal forms using the program *CONTACT* (Collaborative Computational Project, Number 4, 1994).

3. Results and discussion

3.1. The overall structure of ErcA and its complexes with aspartic and glutamic acids

The three-dimensional structure of free ErcA has been described previously (Kislitsyn *et al.*, 2006). The amino-acid sequence of ErcAA and a stereoview of its structure are shown in Figs. 1(*a*) and 1(*b*), resepectively. The overall fold of the polypeptide chain in ErcA and in the ErcAA and ErcAG complexes corresponds to that of an α/β-protein. Identical folds have been observed in other related L-asparaginases (Ehrman *et al.*, 1971; Swain *et al.*, 1993; Lubkowski *et al.*, 2003). Like other structurally characterized L-asparaginases, ErcA functions as a tetramer (Fig. 1*c*) consisting of four identical subunits with approximate 222 symmetry (tetramer *ABEF* here). Each subunit contains 327 amino-acid residues and is composed of 14 β-strands and eight α-helices distributed between the N-terminal and C-terminal domains (Figs. 1*a* and 1*b*). All subunits of the tetrameric molecule of L-asparaginase show a stable and rigid conformation: the r.m.s. deviations between C^{α} atoms of all monomers in the asymmetric units of ErcAA (1.9 Å), ErcAA (2.1 Å) and ErcAG do not exceed 0.21, 0.28 and 0.40 Å, respectively.

Two subunits of L-asparaginase are combined into a so-called 'intimate dimer' that possesses two fully organized active sites (Swain *et al.*, 1993). A distinguishing feature of L-asparaginases is the presence of a left-handed crossover between strands β4 and β5 (residues 119–152 in ErcAA). This type of protein fold is rather rarely observed in protein structures, but is typical of L-asparaginases (Miller *et al.*, 1993). The residues of the left-handed crossover reside at the interface between the intimate dimers, close to the noncrystallographic twofold axis which relates the subunits *AF* and *BE* into a tetramer. Providing a substantial part of the interface between dimers in the proximity of the active sites, this crossover makes a significant contribution to the stabilization of the tetrameric structure.

3.2. Formation of the intimate dimers and tetramer

A network of hydrogen bonds responsible for the formation of intimate dimers (*AE*, *BF*, *DH*, *CG*) was detected and analyzed. Two adjacent monomers form a very strong complex. Polar fragments of the 19 amino-acid residues from each monomer that take part in the intersubunit hydrogen bonds become inaccessible to the solvent upon dimer formation. In most cases the hydrogen bonds are formed between main-chain–main-chain or main-chain–side-chain atoms of corresponding subunits; 11 of them are formed by strongly conserved amino-acid residues. The bond distances are approximately equal in the various intimate dimers.

Each tetramer in the asymmetric units of the ErcAA and ErcAG crystals is stabilized by 22 hydrogen bonds. The most important bonds arise between Ser128, Ala129 and Met133 of NCS-related chains of neighbouring subunits. The hydroxyl group of the Ser128 (Ser128′) side chain is hydrogen bonded to the O atom of the Ala129′ (Ala129) main chain and the N atom of the main chain of Met133′ (Met133) of the corresponding monomer (Fig. 2). Ser128 and Ala129 are strongly conserved residues. Being in an extended conformation, they participate in the formation of an intersubunit four-stranded antiparallel β-sheet. Owing to the formation of hydrogen bonds to the side chains of the adjacent residues 119–121, this segment of the interface provides the rigid conformation of the amino-acid residues nearest to the active-site area. It is possible to suggest that these hydrogen bonds make the tetramer functionally active. It is worth noting that residues Ala119, Ala120, Met121, Ser128, Ala129 and Met133 belong to the left-handed crossover region.

As mentioned above, the tetrameric structure is necessary for the activity of the enzyme. The formation of the tetrameric structure of L-asparaginase intensifies the reactive ability of this enzyme. When the tetrameric structure is formed, part of

the dimer surface becomes unavailable to substrates. In the case of L-asparaginase, the ratio of the active-site area to the area of the surface of the tetrameric structure increases by up to 20% in comparison with that for the dimeric structure. This results in an increase in the number of effective collisions with substrates.

3.3. Active-site area

Similar to other related asparaginases (Swain *et al.*, 1993; Miller *et al.*, 1993; Lubkowski *et al.*, 1996), each of the four active sites in ErcA is formed by two subunits combined into intimate dimers. Two active sites of each dimer are arranged between the N-terminal domain of one subunit and the C-terminal domain of another. The N-terminal domain contains eight active-site residues: Thr15, Tyr29, Ser62, Glu63, Thr95, Asp96, Ala120 and Lys168. Only one residue (Ser254) that belongs to the neighbouring subunit resides in the C-terminal domain. The active site of ErcA is characterized by features that are common to homologous asparaginases. The amino-acid residues of the active site are conserved in asparaginases and, with the exceptions of Ser62 and Glu63, are located in irregular parts of the polypeptide chain. However, these irregular regions are either adjacent to the regions of intersubunit contacts or are involved in these contacts. For example, Thr97, which is adjacent to the active-site residue Asp96, participates in the hydrogen-bond network, binding dimers *AF* and *BE* into a tetramer. Small glycine residues precede the majority of the active-site residues (Fig. 1*a*). The side chains of the active-site residues are involved in the hydrogen-bond network and interact with each other directly or *via* water molecules. The hydrogen-bond network is conserved in the related asparaginases and is probably important for enzyme action (Palm *et al.*, 1996; Lubkowski *et al.*, 2003). It has been shown that Thr15 acts as a primary nucleophile which attacks the C atom of the substrate amide group, whereas Tyr29 holds the attacking nucleophile in the most favourable position. These two residues, which play a key role in the enzyme activity, are located in the flexible loop that includes residues 14–33 (Aghaiypour *et al.*, 2001*a*). This mobile loop covers the active-site cavity; its movement is able to close or open the entrance to the active-site area. The temperature factors of the residues involved in the flexible loop exceed the average *B* value of the molecule.

Although only one residue of the C-terminal domain directly participates in the formation of each active site, part of the polypeptide chain of the C-terminal domain (residues 287–290) is located in close proximity to the flexible loop of the N-terminal domain and residues Asp287, Gly289 (Glu289 in ErchA) or Gln290 (Leu290 in ErchA) can have a pronounced effect on the entrance of the substrate into the active-site cavity. In addition, residues 282–291 of the C-terminal domain represent the major linear epitope, which determines the antigenic properties of the enzyme (Moola *et al.*, 1994). Thus, the difference in the amino-acid sequence in this region between ErcA and ErchA may be functionally important.

The configuration of the polypeptide chain in region Gln280–Phe291 in EcAA differs from that of the *Erwinia* strain. In EcAA Glu283 hinders the entrance to the active-site area, so its accessibility to the larger substrate should be reduced. It correlates well with the higher specific activity of ErcA relative to EcA. At the same time, the increased accessibility of the ErcA active site provides the higher glutaminase activity of this enzyme.

3.4. Binding of L-aspartate and L-glutamate

It is known that L-asparaginase is able to bind both aspartic and glutamic acids at pH values lower than 5. Moreover, at low pH values aspartic acid binds to the enzyme as tightly as asparagine and serves as a substrate of L-asparaginase. The latter catalyzes oxygen exchange between the side-chain carboxylic group of aspartate and water (Howard & Carpenter, 1972; Rohm & Van Etten, 1986; Aghaiypour *et al.*, 2001*b*). Inspection of the electron-density maps of ErcAA and ErcAG allowed us to locate aspartate and glutamate molecules in all the active sites of the tetramer (Figs. 3*a* and 3*b*). The positions of the bound ligands are identical in all fully occupied sites.

Binding of the aspartate resulted in a significant reduction in the mobility of the active-site residues, especially the mobility of the flexible-loop residues 17–33. Electron density is only absent for the first two amino-acid residues, which were also not localized in the structures of related enzymes (Lubkowski *et al.*, 2003). Superposition of ErcAA and free ErcA (r.m.s.d. = 1.2 Å) reveals the shift of Tyr29 from

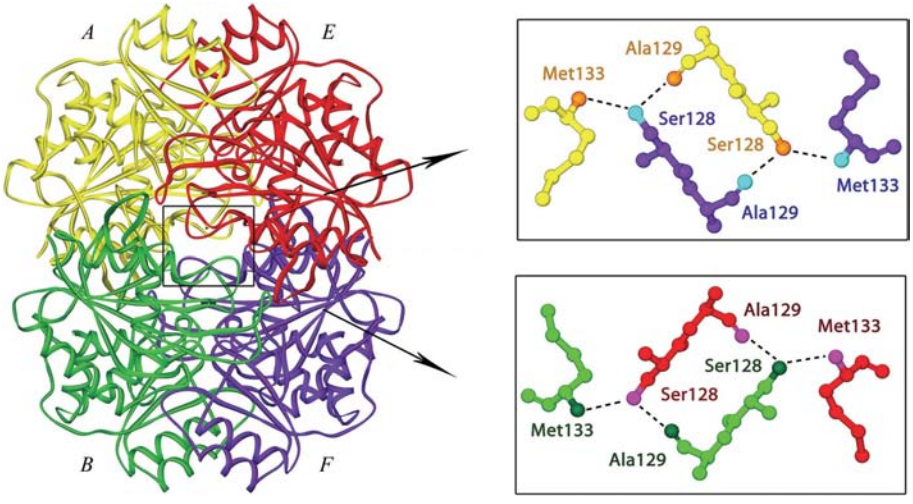

Figure 2
Contact region between the intimate dimers. Part of the antiparallel β-sheet formed between the subunits of two different intimate dimers is shown.

Table 2
Binding of various substrates by L-asparaginases.

Atom	ErcAA (L-aspartic acid)	ErchAAD (D-aspartic acid)	ErcAG (L-glutamic acid)	EchrAG (L-glutamic acid)	EcoAA (L-aspartic acid)	Aspartyl-EcA (L-aspartic acid)	ErchADON-L (L-DON)	ErchADON-D (D-DON)
N	Asp96 OD2 (2.83)	Asp96 OD2 (2.73)	Asp96 OD2 (2.94)	Asp96 OD2 (2.70)	Asp90 OD2 (3.00)	Asp90 OD2 (2.62)	Asp96 OD2 (2.72)	Asp96 OD2 (3.04)
	Glu63 OE1 (2.97)	Glu63 OE1 (2.84)	Glu63 OE1 (2.72)	Glu63 OE1 (2.59)	Gln59 OE1 (2.71)	Gln59 OE1 (2.50)	Glu63 OE1 (2.88)	Glu63 OE1 (2.76)
					Glu283 OE2 (2.46)	Glu283 OE2 (2.86)		
O	Asp96 N (3.12)	Asp96 N (3.12)			Asp96 N (3.24)			Asp96 N (3.08)
	Ser62 OG (2.29)	Ser62 OG (2.29)	Ser62 OG (2.25)	Ser62 OG (2.32)	Ser58 OG (2.41)	Ser58 OG (2.46)	Ser62 OG (2.38)	Ser62 OG (2.21)
	Thr95 N (3.25)				Thr89 N (3.24)			
OXT	Ser62 N (2.84)	Thr95 N (2.81)	Ser62 N (2.92)	Ser62 N (3.00)	Ser58 N (2.68)	Ser58 N (2.81)	Ser62 N (2.67)	Ser62 N (2.84)
O2	Thr95 OG1 (2.75)	Ser62 N (2.79)	Thr95 OG1 (2.52)	Thr95 OG1 (2.80)	Thr89 OG1 (2.65)	Covalent bond with Thr15 OG	Thr95 OG1 (2.63)	Thr95 OG1 (2.59)
	Ala120 O (3.14)			Thr95 N (2.83)	Ala114 O (3.14)		Ala120 O (3.04)	Ala120 O (3.22)
O1	Thr15 N (3.15)		Thr15 N (3.21)	Thr15 N (2.61)	Thr12 N (2.77)	Thr12 N (2.74)		
	Thr95 N (2.96)						Thr89 N (2.94)	Thr89 N (3.07)

the ligand as a result of the binding of L-aspartate. The distance between the C^{α} atoms of Tyr29 in the superimposed structures is 2.6 Å; the corresponding distance between the hydroxyl O atoms of Tyr29 is 2.4 Å.

The surroundings of the aspartate molecule in ErcAA are very similar to its surroundings in other known L-asparaginase complexes (Figs. 3*a* and 3*b*). The α-NH_3^+ group forms hydrogen bonds to the side-chain carboxyl O atoms of Asp96 and Glu63 and to the water molecule involved in the active-site hydrogen-bond network. According to Aghaiypour *et al.* (2001*b*), the α-amino group of the aspartic acid is the main determinant of specificity; substrates that lack it cannot be productively bound by some bacterial asparaginases. The α-amino group provides the correct orientation for processing the substrate molecule (Lubkowski *et al.*, 2003).

The α-COOH group of aspartate also interacts with the enzyme in a highly conserved fashion. One of its O atoms is hydrogen bonded to the amide group of Asp96, the main-chain N atom of Thr95 and the γ-OH group of Ser62, while the other forms hydrogen bonds to the amide group of Ser62. It has been suggested (Aghaiypour *et al.*, 2001*b*) that its α-COOH group is responsible for substrate binding.

The δ-COOH group of aspartate is positioned close to the catalytically important residues. One of the O atoms (OD2) of the side-chain carboxylic group binds the OG1 atom of Thr95, the main-chain O atom of Ala120 and water molecule W2 (Fig. 3*a*); the second (OD1) binds the main-chain N atoms of Thr15 and Thr95, and water molecule W1.

In general, L-aspartic acid forms ten hydrogen bonds to the enzyme that are inaccessible to the solvent; six are formed to the main-chain atoms of L-asparaginase (Table 2 and Fig. 3*a*).

The glutamate in ErcAG mostly interacts with the same group of atoms as aspartate. However, the relative orientation of the contacting groups of the enzyme structure differs slightly for the two substrates. Similar to in ErchAG (Aghaiypour *et al.*, 2001*a*), the δ-carboxyl group of L-aspartate

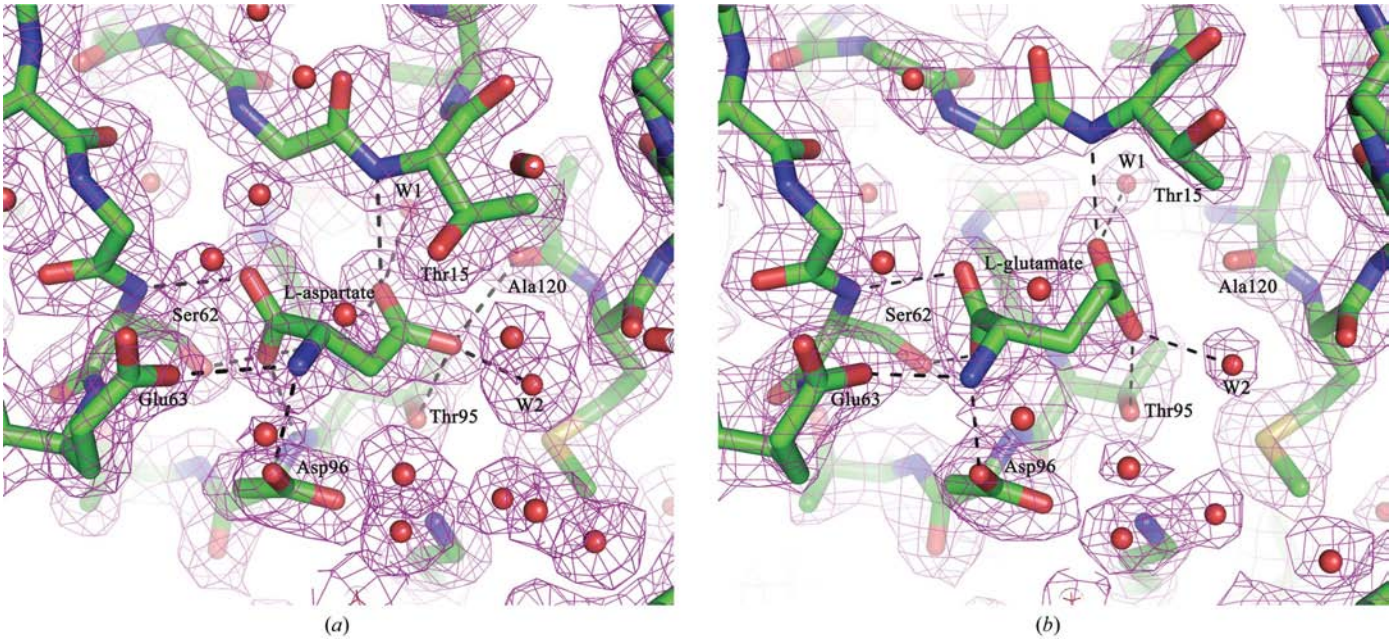

Figure 3
Aspartate (*a*) and glutamate (*b*) bound in the active site of ErcAA. W1 and W2 are the conserved water molecules nearest to the ligand.

and the ε-carboxyl group of L-glutamate in ErcAG are close to each other but lie in perpendicular planes (Fig. 3). In comparison with aspartic acid, there is a reduced number of solvent-inaccessible hydrogen bonds between L-glutamic acid and ErcA (Figs. 3*a* and 3*b*). The hydrogen bond between the glutamate O atom and the main-chain N atom of Thr95 that was found in ErchrAG is absent in ErcAG. In both complexes the interaction with the Ala120 main-chain O atom is lost. According to Aghaiypour *et al.* (2001*a*), the absence of these interactions results in slower L-glutamate hydrolysis. It is worth noting that in both the ErchAG and ErcAG complexes residues 17–33 of the flexible loop are disordered and are not seen in the electron-density map.

Amino-acid residues Thr15 and Tyr29 of the active site located in the flexible loop change their positions upon substrate binding. The conformation of Thr15 depends on the substrate and the specificity of the enzyme for this substrate. The Thr15 side chain of ErcAG and ErchAG is rotated outwards from the substrate in comparison with the conformation of Thr15 in ErcAA and EcAA. It is interesting to note that in the L-asparaginases from *Acinetobacter glutaminasificans* and *Pseudomonas* 7A, which catalyze the hydrolysis of both L-asparagine and L-glutamine with comparable efficiency (Aghaiypour *et al.*, 2001*b*), the Thr15 side chains have the same conformation as in the L-aspartate-specific ErcAA, ErchAS and ErcA. It is possible that the conformation of Thr15 correlates with the specificity of the substrate.

3.5. Water molecules in the vicinity of bound aspartate in ErcAA

Two water molecules, W1 and W2 (Fig. 3*a*), are located close to the δ-COOH group of the aspartic acid in ErcAA. The conserved hydrogen bonds formed by the participation of these molecules are an inherent feature of the active site of L-asparaginase and are therefore essential for the maintainance of enzyme activity (Lubkowski *et al.*, 2003). Such water molecules are found in similar positions in a number of L-asparaginases (Palm *et al.*, 1996; Lubkowski *et al.*, 1996, 2003; Aghaiypour *et al.*, 2001*b*; Sanches *et al.*, 2003; Jakob *et al.*, 1997; Miller *et al.*, 1993).

Water W1 forms hydrogen bonds to the main-chain N atoms of Ala120 and Ile16 and the main-chain O atoms of Ala120 and His93 as well as to the L-aspartate. Thr95 is important for enzyme activity, while Ala120 provides the removal of product after reaction (Aghaiypour *et al.*, 2001*a*). Ile16 is located at the beginning of the flexible loop. W1 may be important for the maintenance of a suitable polypeptide-chain conformation in the functionally important region. On the other hand, a water molecule in such surroundings can serve as a proton donor during substrate hydrolysis and water exchange, taking part in stabilization of the tetrahedral intermediate (Miller *et al.*, 1993). It is worth noting that removing a proton from a water molecule converts it to a hydroxyl anion, which is a strong nucleophile. Thus, it is possible that the hydroxyl anion in this site serves as a nucleophile upon deacylation of the covalent intermediate formed by the previous step of enzymatic hydrolysis of the substrate.

The W2 molecule has in its nearest coordination sphere the main-chain O atom of Met121, which adjoins the active-site residue Ala120. The latter binds to the side-chain N atom of Lys168, which is important for enzyme activity (Swain *et al.*, 1993), *via* one of the water molecules. W2 is not found in EcAG and ErchAG, as well as in some of the subunits of the ErcAG molecule. This can be explained by partial distortion of the hydrogen-bond network upon binding of the less specific substrate.

3.6. Comparison of ErcAA with several derivatives of related asparaginases

Comparison of ErcAA with known derivatives of related L-asparaginases reveals the conformation changes that accompany the catalyzed reaction.

It is known (Howard & Carpenter, 1972) that L-asparaginase hydrolyzes D-asparagine with a significantly lower rate than L-asparagine and even L-glutamine. The structure of L-asparaginase bound to D-aspartate has been solved for ErchA (Aghaiypour *et al.*, 2001*a*). It was shown that the binding of D-aspartate, like the binding of L-glutamate, is accompanied by disordering of the flexible loop (residues 17–34). Superpositioning of ErcAAL and ErchAAD reveals that three atoms of both ligands (the C^{α} atom, the N atom of the α-NH_3^+ group and one of the O atoms of the α-COOH group) occupy very similar positions and bind to the same residues. The side chains of the D- and L-aspartates in the superimposed structures are strongly displaced from each other. As a result, the δ-COOH group of D-aspartate is distant from the primary Thr15 nucleophile and one O atom of the δ-COOH group (O2 in Table 2) simulates the position of the O atom (OXT) of the α-COOH group of L-aspartate.

Although water molecules W1 and W2 in both structures retain their positions inside the active site, their positions in relation to the bound ligand are different. W2 in ErchAAD is removed from the D-aspartate side chain. W1 in ErchAAD is bound to one of the O atoms of the α-COOH group instead of δ-COOH in ErcAAL. Such a water position makes the processing of D-asparagine difficult. Moreover, in such a position the hydrolysis of the α-amide of the aspartic acid seems to be more favourable. However, it is necessary to remember that the orientation of D-asparagine during the course of the reaction could be different. Because productive binding of D-aspartate is very hindered, its hydrolysis occurs at a very slow rate and is accompanied by disordering of the flexible loop. It is probably that the disordering of the flexible loop allows the enzyme to adopt a conformation suitable for D-aspartate processing.

It is agreed that hydrolysis of asparagine by L-asparaginase proceeds through the double-displacement reaction (Rohm & Etten, 1986; Ehrman *et al.*, 1971). Initial nucleophilic attack on the amide C atom of asparagine or glutamine by the enzyme leads to a tetrahedral intermediate which breaks down to form an acyl-enzyme intermediate and generates an ammonia

molecule as a byproduct. This intermediate is then attacked by a secondary nucleophile, normally water, releasing the product (Rohm & Van Etten, 1986). Because protonated aspartate serves as a substrate of L-asparaginase, the structure of ErcAA represents the state of the enzyme after substrate/product binding.

The known structures of *Er. chrysanthemi* L-asparaginase and *Pseudomonas* 7A glutaminase-asparaginase (Aghaiypour *et al.*, 2001*b*; Ortland *et al.*, 2000) inhibited with 6-diazo-5-oxo-L-norleucine (DON) and the structure of mutant T89V *E. coli* L-asparaginase acylated by L-aspartate (Palm *et al.*, 1996) can be considered as analogues of the tetrahedral and the covalent intermediates arising during the reaction, respectively. Comparison of ErcAA with both of these structures reveals the conformational changes in the enzyme active site that accompany the reaction. A superposition of the active-site fragments of ErcAA and ErchA in complex with DON and T89V EcoAA is shown in Fig. 4. DON, an antibiotic isolated from *Streptomyces*, is a diazo analogue of L-glutamic acid and acts as a suicide inhibitor of glutaminase-asparaginases. DON has been shown (Ortland *et al.*, 2000) to form two covalent ether bonds with the enzyme *via* the hydroxyl groups of Thr15 and Tyr29. As a result, the C atom linked to these O atoms adopts a tetrahedral configuration. Superposition of ErchA inhibited by DON and ErcAA reveals a striking change in the positions of the residues of the flexible loop, especially Tyr29. The latter is displaced by a distance of about of 4.0 Å in the direction towards Thr15. Thus, in the complex of L-asparaginase with DON, the closed conformation of the active site is realised. The mutant form of *E. coli* T89V L-asparaginase in which Thr12 is acylated by an aspartyl moiety serves as a suitable model of the covalent intermediate. Comparison of the ErcAA and *E. coli* mutant structures shows that the active site is only slightly rearranged and that the aspartyl residue in the *E. coli* enzyme and the aspartic acid in ErcAA occupy very similar positions. In the *E. coli* mutant form the most drastic alterations take place in the positions of the amino-acid residues of the flexible loop. Tyr25 (Tyr29 in ErcA) in the β-aspartyl enzyme shifts towards the β-aspartyl moiety and rotates. The distance between the tyrosine phenolic O atom and the ether O atom of the β-aspartyl groups becomes 2.84 Å, whereas the distance between the phenolic O atom of Tyr29 and the nearest O atom of the aspartate α-COOH group in ErcAA is 7.12 Å. Comparison of free ErcA and ErcAA shows that Tyr29 is shifted away from the ligand. The same picture is observed on comparing ErcA and ErchA (Lubkowski *et al.*, 2003), in which an SO_4^{2-} ion occupies the position of the aspartate O atom.

Thus, we can see that the accessibility of the active site is altered during the course of the catalytic reaction. The accessibility is regulated by the movement of residues of the flexible loop, especially the essential tyrosine. The loop is able to move in the direction towards the ligand, producing a closed conformation of the active site. The largest shift of Tyr29 towards the ligand is observed during the step involving the formation of the tetrahedral intermediate. L-Aspartic acid fits ideally into the active-site cavity without distortion of the active-site flexible loop, although a shift of Tyr29 in the direction from the ligand takes place (Fig. 5). The closed conformation of the active site is only attained for specific substrates. The accommodation of less specific substrates is accompanied by disordering of the flexible loop and, as a consequence, by some distortion of the hydrogen-bond network. Movement of the active-site flexible loop in the

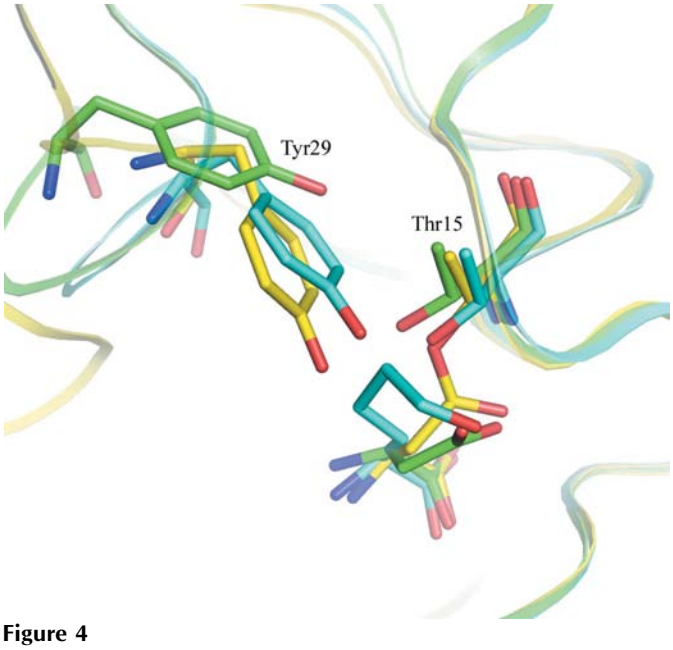

Figure 4
The shift of Tyr29 (Tyr25) in different forms of L-asparaginase. A superposition of the active-site fragments of ErcAA (green), ErchA in complex with DON (light blue) and aspartyl-EcA (yellow) is shown.

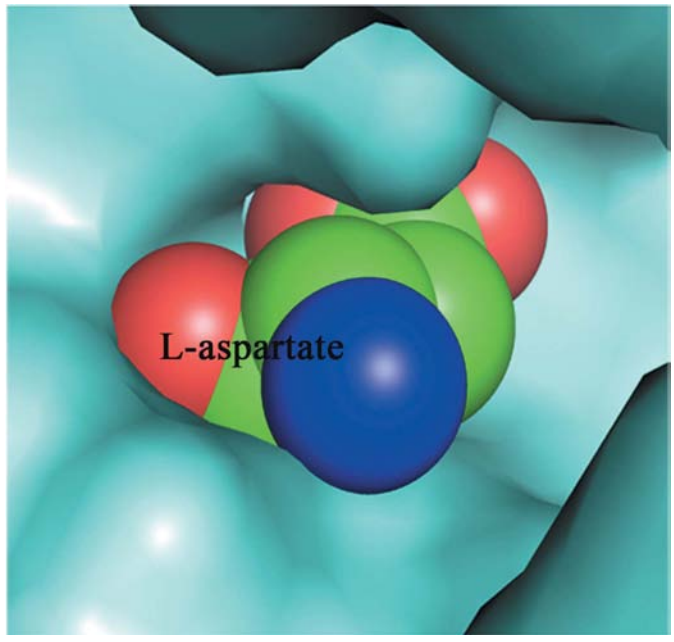

Figure 5
The surface of the ErcA active site with a molecule of aspartic acid, covered from the top by the residues of the flexible loop. L-Aspartate atoms are shown as spheres. The sphere sizes correspond to van der Waals radii. Aspartic acid is complementary to the active-site surface.

direction of the substrate is observed when the acyl-enzyme or tetrahedral intermediate are formed and movement away from the substrate occurs when the product binds to the free enzyme (Fig. 4). It is possible that the mutation of the residues of the flexible loop could change the accessibility of the active site and influence the enzyme specificity.

This work was supported by RFBR (grant 04-04-49085). We thank Professor N. N. Sokolov for providing the purified preparation of *Er. carotovora* L-asparaginase.

References

Aghaiypour, K., Wlodawer, A. & Lubkowski, J. (2001*a*). *Biochemistry*, **40**, 5655–5664.

Aghaiypour, K., Wlodawer, A. & Lubkowski, J. (2001*b*). *Biochim. Biophys. Acta*, **1550**, 117–129.

Brünger, A. T., Adams, P. D., Clore, G. M., DeLano, W. L., Gros, P., Grosse-Kunstleve, R. W., Jiang, J.-S., Kuszewski, J., Nilges, M., Pannu, N. S., Read, R. J., Rice, L. M., Simonson, T. & Warren, G. L. (1998). *Acta Cryst.* D**54**, 905–921.

Carlsson, H., Stockelberg, D., Tengborn, L., Braide, I., Cameskog, J. & Kutty, J. (1995). *Eur. J. Haematol.* **55**, 289–293.

Collaborative Computational Project, Number 4 (1994). *Acta Cryst.* D**50**, 760–763.

Derst, C., Henseling, J. & Rohm, K. H. (2000). *Protein Sci.* **9**, 2009–2017.

Ehrman, M., Cedar, H. & Schwartz, J. H. (1971). *J. Biol. Chem.* **246**, 88–94.

Emsley, P. & Cowtan, K. (2004). *Acta Cryst.* D**60**, 2126–2132.

Hooft, R. W. W., Vriend, G., Sander, C. & Abola, A. A. (1996). *Nature (London)*, **381**, 272.

Hortobagyi, G. N., Yap, H. Y., Wiseman, C. L., Blumenshain, G. R., Buzdar, A. U., Legha, S. S., Gutterman, J. U., Hersh, E. M. & Bodey, G. P. (1980). *Cancer Treat. Rep.* **64**, 157–159.

Howard, J. B. & Carpenter, F. J. (1972). *J. Biol. Chem.* **217**, 1020–1030.

Jakob, C. G., Lewinski, K., Lacount, M. W., Roberts, J. & Lebioda, L. (1997). *Biochemistry*, **36**, 923–931.

Jones, T. A., Zou, J.-Y., Cowan, S. W. & Kjeldgaard, M. (1991). *Acta Cryst.* A**47**, 110–119.

Kislitsyn, Yu. A., Kravchenko, O. V., Nikonov, S. V. & Kuranova, I. P. (2006). *Crystallogr. Rep.* **51**, 811–816.

Krasotkina, Ju., Borisiva, A. A., Gervaziev, Yu. V. & Sokolov, N. N. (2004). *Biotechnol. Appl. Biochem.* **39**, 215–221.

Laskowski, R. A., MacArthur, M. W., Moss, D. S. & Thornton, J. M. (1993). *J. Appl. Cryst.* **26**, 283–291.

Lubkowski, J., Dauter, M., Aghaiypour, K., Wlodawer, A. & Dauter, Z. (2003). *Acta Cryst.* D**59**, 84–92.

Lubkowski, J., Palm, G. J., Gilliland, G. L., Derst, C., Rohm, K.-H. & Wlodawer, A. (1996). *Eur. J. Biochem.* **241**, 201–207.

Lubkowski, J., Wlodawer, A., Ammon, H. L., Copeland, T. D. & Swain, A. L. (1994). *Biochemistry*, **33**, 10257–10265.

Lubkowski, J., Wlodawer, A., Housset, D., Weber, I. T., Ammon, H. L., Murphy, K. C. & Swain, A. L. (1994). *Acta Cryst.* D**50**, 826–832.

Miller, M., Rao, J. K. M., Wlodawer, A. & Gribskov, M. R. (1993). *FEBS Lett.* **238**, 275–279.

Moola, Z. B., Scawen, M. D., Atkinson, T. & Nicholls, D. J. (1994). *Biochem. J.* **302**, 921–927.

Murshudov, G. N., Vagin, A. A., Lebedev, A., Wilson, K. S. & Dodson, E. J. (1999). *Acta Cryst.* D**55**, 247–255.

Navaza, J. (1994). *Acta Cryst.* A**50**, 157–163.

Ortland, E., LaCount, M. W., Lewinski, K. & Lebioda, L. (2000). *Biochemistry*, **39**, 1199–1204.

Otwinoski, Z. & Minor, W. (1997). *Methods Enzymol.* **276**, 307–326.

Palm, G. J., Lubkowski, J., Derst, C., Schleper, S., Rohm, K. H. & Wlodawer, A. (1996). *FEBS Lett.* **390**, 211–216.

Polikarpov, I., de Oliveira, R. T. & Abrahão-Neto, J. (1999). *Acta Cryst.* D**55**, 1616–1617.

Roberts, J., Schmid, F. A. & Rosenfeld, H. J. (1979). *Cancer Treat. Rep.* **63**, 1045–1054.

Rohm, K. H. & Van Etten, R. L. (1986). *Arch. Biochem. Biophys.* **244**, 128–136.

Sanches, M., Barbosa, J. A. R. G., de Oliveira, R. T., Abrahão Neto, J. A. & Polikarpov, I. (2003). *Acta Cryst.* D**59**, 416–422.

Storoni, L. C., McCoy, A. J. & Read, R. J. (2004). *Acta Cryst.* D**60**, 432–438.

Stura, E. A. & Wilson, I. A. (1991). *J. Cryst. Growth.* **110**, 270–282.

Swain, A. L., Jaskolski, M., Housset, D., Rao, J. K. M. & Wlodawer, A. (1993). *Proc. Natl Acad. Sci. USA*, **90**, 1474–1478.

Wikman, L. E. K., Krasotkina, J., Kuchumova, A., Sokolov, N. N. & Papageorgiou, A. C. (2005). *Acta Cryst.* F**61**, 407–409.

Wo, M. C., Arimura, G. K. & Yunis, A. A. (1978). *Int. J. Cancer*, **22**, 728–733.